NUWC-NL Technical Report 10,165
15 October 1992

A Nonconforming Approximate Solution to a Specially Orthotropic Axisymmetric Thin Shell Subjected to a Harmonic Displacement Boundary Condition

Andrew J. Hull
Submarine Sonar Department

Naval Undersea Warfare Center Detachment
New London, Connecticut

PREFACE

This report was prepared under NUWC Project No. 15600, *TB-29 Towed Array Development Program,* Principal Investigator W. A. Birtcher (Code 2143). The sponsoring activity is the Program Executive Office, Submarine Combat and Weapon Systems, Capt. G. A. Kent.

The technical reviewer for this report was D. A. Hurdis (Code 2141).

The author wishes to thank W. A. Strawderman (NUWC Code 213) and S. A. Austin (NUWC Code 2141) for their assistance with this effort. Appreciation is also extended to Karen Holt (NUWC Code 0211) for her help with the technical editing.

REVIEWED AND APPROVED: 15 OCTOBER 1992

F. J. Kingsbury

F. J. Kingsbury
Head, Submarine Sonar Department

REPORT DOCUMENTATION PAGE

Form Approved
OMB No. 0704-0188

1. AGENCY USE ONLY *(Leave blank)*

2. REPORT DATE
15 October 1992

3. REPORT TYPE AND DATES COVERED
Progress

4. TITLE AND SUBTITLE
A Nonconforming Approximate Solution to a Specially Orthotropic Axisymmetric Thin Shell Subjected to a Harmonic Displacement Boundary Condition

5. FUNDING NUMBERS

6. AUTHOR(S)
Andrew J. Hull

7. PERFORMING ORGANIZATION NAME(S) AND ADDRESS(ES)
Naval Undersea Warfare Center
New London, Connecticut 06320

8. PERFORMING ORGANIZATION REPORT NUMBER
TR 10,165

9. SPONSORING/MONITORING AGENCY NAME(S) AND ADDRESS(ES)
Program Executive Office
Submarine Combat and Weapons Systems
Washington, DC 20362-5103

10. SPONSORING/MONITORING AGENCY REPORT NUMBER

11. SUPPLEMENTARY NOTES

12a. DISTRIBUTION/AVAILABILITY STATEMENT
Approved for public release; distribution is unlimited.

12b. DISTRIBUTION CODE

13. ABSTRACT *(Maximum 200 words)*

This report develops an approximate closed form solution to a specially orthotropic axisymmetric cylindrical thin shell subjected to a harmonic boundary condition. Modified Love-Timoshenko shell equations forced by a harmonic boundary condition at one end of the shell and grounded by a mechanical spring at the other are used to formulate this boundary value problem. Each modeled shell is subjected to an axial tension, and a steady state approximate solution is then formulated. The solutions derived here are compared to finite element results and to previous models of the thin shell problem. It is shown that the finite element analysis agrees very closely with the equations derived in this study. It is also shown that the earlier models used to analyze specially orthotropic thin shells produce results that do not agree with the model developed here or with the finite element analysis. Shell configurations evaluated include finite length isotropic, finite length specially orthotropic, semi-infinite length specially orthotropic, and damped finite length specially orthotropic.

14. SUBJECT TERMS
Boundary Value Problem
Closed Form Solution
Cylindrical Thin Shell
Harmonic Displacement Boundary Condition
Orthotropic

15. NUMBER OF PAGES

16. PRICE CODE

17. SECURITY CLASSIFICATION OF REPORT	18. SECURITY CLASSIFICATION OF THIS PAGE	19. SECURITY CLASSIFICATION OF ABSTRACT	20. LIMITATION OF ABSTRACT
UNCLASSIFIED	UNCLASSIFIED	UNCLASSIFIED	SAR

NSN 7540-01-280-5500

Standard Form 298 (Rev. 2-89)
Prescribed by ANSI Std Z39-18
298-102

TABLE OF CONTENTS

		Page
	LIST OF ILLUSTRATIONS	ii
	LIST OF TABLES	ii
1.	INTRODUCTION	1
2.	SYSTEM MODEL	2
3.	A NONCONFORMING APPROXIMATE SOLUTION	5
4.	FINITE ELEMENT ANALYSIS	7
5.	AN ISOTROPIC EXAMPLE	8
6.	A SPECIALLY ORTHOTROPIC EXAMPLE - FINITE LENGTH SHELL	12
7.	A SPECIALLY ORTHOTROPIC EXAMPLE - SEMI-INFINITE LENGTH SHELL	17
8.	A SPECIALLY ORTHOTROPIC EXAMPLE - INCLUSION OF STRUCTURAL DAMPING	23
9.	DISCUSSION	27
10.	CONCLUSIONS	28
11.	REFERENCES	29

LIST OF ILLUSTRATIONS

Figure		Page
1	Laboratory Configuration	2
2	Longitudinal Response of Isotropic Example at $x = 7$ Meters	10
3	Radial Response of Isotropic Example at $x = 7$ Meters	11
4	Longitudinal Response of Specially Orthotropic Example at $x = 16$ Meters	14
5	Radial Response of Specially Orthotropic Example at $x = 16$ Meters Using $\upsilon = 0.0049$ for Equation (34)	15
6	Radial Response of Specially Orthotropic Example at $x = 16$ Meters Using $\upsilon = 0.4900$ for Equation (34)	16
7	Configuration of Semi-Infinite System	18
8	Longitudinal Response of Semi-Infinite Specially Orthotropic Example at $x = 12$ Meters	20
9	Radial Response of Semi-Infinite Specially Orthotropic Example at $x = 12$ Meters Using $\upsilon = 0.0049$ for Equation (39)	21
10	Radial Response of Semi-Infinite Specially Orthotropic Example at $x = 12$ Meters Using $\upsilon = 0.4900$ for Equation (39)	22
11	Longitudinal Response of Damped and Undamped Specially Orthotropic Example at $x = 16$ Meters	25
12	Radial Response of Damped and Undamped Specially Orthotropic Example at $x = 16$ Meters	26

LIST OF TABLES

Table		Page
1	Shell Properties for Isotropic Example	9
2	Shell Properties for Specially Orthotropic Example	13
3	Shell Properties for Specially Orthotropic Semi-Infinite Length Example	19
4	Shell Properties for Specially Orthotropic Damped Example	24

A NONCONFORMING APPROXIMATE SOLUTION TO A SPECIALLY ORTHOTROPIC AXISYMMETRIC THIN SHELL SUBJECTED TO A HARMONIC DISPLACEMENT BOUNDARY CONDITION

1. INTRODUCTION

The design of lightweight, inexpensive, and strong shells is critical to many mechanical systems. The analysis of various types of shells under different loading configurations has been reported by numerous researchers (Naghdi and Berry, 1954; Flugge, 1960; Junger and Feit, 1986; Vinson and Sierakowski, 1987; Qaisi, 1989). In these papers, the governing partial differential equations to evaluate a particular shell are usually developed and then a response is formulated. The response is an equation of motion, which is required to compare test data to analytical models or to solve an inverse problem (i.e., the test is run and the system parameters are identified by the test data.)

In this report, the partial differential equations of an axisymmetric composite thin shell subjected to a harmonic boundary condition are developed. First, the model of a shell subjected to axial tension with a mechanical shaker at the forward end and terminated by a rope to ground at the after end is formulated. The partial differential equations are transformed into ordinary differential equations. An approximate solution to the ordinary differential equations of motion is then derived. The model is verified with comparisons to results from finite element analysis of the same thin shell problem. The model is also compared to a previous model of the system.

The new model corresponds to the testing configuration in the Axial Vibration Test Facility (AVTF) at the Naval Undersea Warfare Center (NUWC), as shown in figure 1. This facility has been designed to provide a simple procedure for testing shells under varying tensions and temperatures.

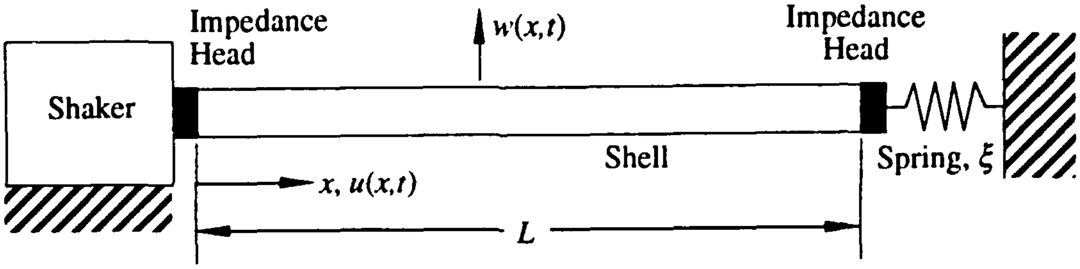

Figure 1. Laboratory Configuration

2. SYSTEM MODEL

The system model is an axisymmetric thin shell with a displacement-driven boundary condition at one end and a mechanically grounded spring at the other end. The governing partial differential equations are modified axisymmetric Love-Timoshenko formulas. The longitudinal (axial) partial differential equation that relates the shells longitudinal acceleration to its axial stress is

$$\rho \frac{\partial^2 u(x,t)}{\partial t^2} = \frac{\partial \sigma_x(x,t)}{\partial x} , \tag{1}$$

where $u(x,t)$ is the axial displacement (m), x is the axial spatial location (m), t is time (s), ρ is the density of the shell (kg/m^3), and $\sigma_x(x,t)$ is the axial stress in the shell (N/m^2). The radial (circumferential) partial differential equation that relates the radial acceleration of the shell to its tension, bending stiffness, and circumferential stress is

$$\rho h \frac{\partial^2 w(x,t)}{\partial t^2} = \frac{T}{2\pi a} \frac{\partial^2 w(x,t)}{\partial x^2} - B \frac{\partial^4 w(x,t)}{\partial x^4} - \frac{h}{a} \sigma_\phi(x,t) , \tag{2}$$

where $w(x,t)$ is the radial displacement (m), h is the shell thickness (m), T is the tension in the shell (N), a is the average radius of the shell (m), B is the bending stiffness of the shell (Nm), and $\sigma_\phi(x,t)$ is the circumferential (hoop) stress (N/m^2). The bending stiffness of the shell is given by the expression

$$B = \frac{E_x h^3}{12} , \tag{3}$$

where E_x is the axial elastic modulus (N/m^2). The longitudinal elastic modulus of a thin shell is related to Young's modulus using the equation

$$E_x = \frac{E}{(1 - \upsilon_{x\phi}\upsilon_{\phi x})} , \tag{4}$$

where E is Young's modulus (N/m^2), $\upsilon_{x\phi}$ is Poisson's ratio relating an axial force to a circumferential displacement, and $\upsilon_{\phi x}$ is Poisson's ratio relating a circumferential force to an axial displacement. The relationship between these two Poissons' ratios will be discussed later in the report.

The dynamic stresses, $\sigma_x(x,t)$ and $\sigma_\phi(x,t)$, are determined by combining two-dimensional stress-strain relations and the strain-displacement relations in cylindrical coordinates. The equation relating the longitudinal stress to the axial and circumferential strain for an axisymmetrical solid is (Jones, 1975)

$$\sigma_x(x,t) = E_x\varepsilon_x(x,t) + \upsilon_{x\phi}E_\phi\varepsilon_\phi(x,t) , \tag{5}$$

where $\varepsilon_x(x,t)$ is the longitudinal strain (dimensionless), E_ϕ is the circumferential modulus (N/m^2), and $\varepsilon_\phi(x,t)$ is the circumferential strain (dimensionless). The longitudinal strain is related to the longitudinal displacement by

$$\varepsilon_x(x,t) = \frac{\partial u(x,t)}{\partial x} \tag{6}$$

and the axisymmetric circumferential strain is related to the circumferential displacement in a thin shell by

$$\varepsilon_\phi(x,t) = \frac{w(x,t)}{a} . \tag{7}$$

Equations (6) and (7) can be inserted into equation (5), which produces an axial stress of

$$\sigma_x(x,t) = E_x\frac{\partial u(x,t)}{\partial x} + \frac{\upsilon_{x\phi}E_\phi w(x,t)}{a} . \tag{8}$$

The equation relating the hoop stress to the circumferential and longitudinal strain for an axisymmetrical solid is (Jones, 1975)

$$\sigma_\phi(x,t) = E_\phi \varepsilon_\phi(x,t) + \upsilon_{\phi x} E_x \varepsilon_x(x,t) \ . \tag{9}$$

Equations (6) and (7) can be inserted into equation (9) to yield a circumferential stress of

$$\sigma_\phi(x,t) = \frac{E_\phi w(x,t)}{a} + \upsilon_{\phi x} E_x \frac{\partial u(x,t)}{\partial x} \ . \tag{10}$$

Equation (8) is now differentiated with respect to x and inserted into equation (1), which gives

$$\rho \frac{\partial^2 u(x,t)}{\partial t^2} = E_x \frac{\partial^2 u(x,t)}{\partial x^2} + \frac{\upsilon_{x\phi} E_\phi}{a} \frac{\partial w(x,t)}{\partial x} \ . \tag{11}$$

Equation (10) is next inserted directly into equation (2) yielding

$$\rho h \frac{\partial^2 w(x,t)}{\partial t^2} = -B \frac{\partial^4 w(x,t)}{\partial x^4} + \frac{T}{2\pi a} \frac{\partial^2 w(x,t)}{\partial x^2} - \frac{h E_\phi}{a^2} w(x,t) - \frac{h \upsilon_{\phi x} E_x}{a} \frac{\partial u(x,t)}{\partial x} \ . \tag{12}$$

Equations (11) and (12) are the two-dimensional axisymmetric equations of motion for the specially orthotropic shell.

The harmonic boundary condition in the axial direction at $x = 0$ is modeled as

$$u(0,t) = U_0 e^{i\omega t} \ , \tag{13}$$

where U_0 is the amplitude of the displacement at the boundary (m), i is the square root of -1, and ω is frequency (rad/s). The boundary condition in the axial direction at $x = L$ is modeled as a spring connected at one end to the shell and to mechanical ground (zero displacement) at the other end. This equation is derived as follows by equating the force at the end of the shell to the force in the spring:

$$A E_x \frac{\partial u(L,t)}{\partial x} = -\xi u(L,t) \tag{14}$$

where A is the cross-sectional area of the shell (m^2) and ξ is the spring constant (N/m). The boundary conditions in the radial direction are zero displacement and zero shear force (Junger and Feit, 1986). These conditions are written as

$$w(0,t) = 0 \ , \tag{15}$$

$$w(L,t) = 0 \ , \tag{16}$$

$$\frac{\partial w(0,t)}{\partial x} = 0 \ , \tag{17}$$

and

$$\frac{\partial w(L,t)}{\partial x} = 0 \ . \tag{18}$$

Although the boundary conditions given by equations (15) - (18) are not used in the final analysis, they are included here for a complete treatment of the theory. The effect of not using these boundary conditions is discussed later in the report.

It should be noted that the previous equations used to model this system are (Chase, 1975)

$$\rho \frac{\partial^2 u(x,t)}{\partial t^2} = E_x \frac{\partial^2 u(x,t)}{\partial x^2} + \frac{\upsilon \alpha E_x}{a} \frac{\partial w(x,t)}{\partial x} \tag{19}$$

and

$$\rho h \frac{\partial^2 w(x,t)}{\partial t^2} = -B \frac{\partial^4 w(x,t)}{\partial x^4} + \frac{T}{2\pi a} \frac{\partial^2 w(x,t)}{\partial x^2} - \frac{h\alpha^2 E_x}{a^2} w(x,t) - \frac{h\upsilon \alpha E_x}{a} \frac{\partial u(x,t)}{\partial x} \ , \tag{20}$$

with

$$\alpha^2 = \frac{E_\phi}{E_x} \ , \tag{21}$$

where α and α^2 are both dimensionless quantities. Equations (11) and (12), derived earlier in this section, will be compared to equations (19) and (20) as well as to results from finite element analysis of several thin shell problems.

3. A NONCONFORMING APPROXIMATE SOLUTION

An approximate closed form solution can be developed for the partial differential equations and the boundary conditions in the longitudinal direction. This calculation assumes that the time and space modes of the system will decouple. A steady state solution is also of interest, because it allows the displacements to be written as

$$u(x,t) = U(x)e^{i\omega t} \tag{22}$$

and

$$w(x,t) = W(x)e^{i\omega t} \ . \tag{23}$$

A second assumption, which presumes that the dynamic coupling from the radial equation into the longitudinal equation is negligible, results in an approximate solution to the problem. It will be shown that, based on the selected loading condition on the structure, this premise is reasonable. If the radial displacement derivative term is dropped and equation (22) is used, equation (11) can be rewritten as

$$\frac{d^2U(x)}{dx^2} + k^2U(x) = 0 \tag{24}$$

with

$$k = \frac{\omega}{\sqrt{\dfrac{E_x}{\rho}}} \ , \tag{25}$$

where k is the extensional wavenumber (rad/m). The general solution to equation (24) is

$$U(x) = G\cos kx + H\sin kx \ . \tag{26}$$

The boundary conditions from equations (13) and (14) are now applied to equation (26) to solve for the constants G and H resulting in

$$\frac{U(x)}{U_0} = \cos kx + \left(\frac{AE_x k\sin kL - \xi\cos kL}{AE_x k\cos kL + \xi\sin kL}\right)\sin kx \ , \tag{27}$$

which is the closed form approximate solution to the axial equation of motion.

The radial equation of motion (12) is now rewritten using equations (22), (23), and the first derivative of equation (27) as

$$B\frac{d^4W(x)}{dx^4} - \frac{T}{2\pi a}\frac{d^2W(x)}{dx^2} + \left(\frac{hE_\phi}{a^2} - \omega^2\rho h\right)W(x) =$$

$$\frac{U_0 h\upsilon_{\phi x}E_x k}{a}(\sin kx - H\cos kx) \ , \tag{28}$$

where

$$H = \frac{AE_x k \sin kL - \xi \cos kL}{AE_x k \cos kL + \xi \sin kL} \ . \tag{29}$$

Equation (28) is now a nonhomogeneous ordinary differential equation whose forcing function was derived from the axial equation of motion. The particular solution to equation (28) is of the form

$$W(x) = M \cos kx + N \sin kx \ . \tag{30}$$

Equation (30) can be differentiated two and four times with respect to x and then inserted into equation (28), yielding the radial displacement of

$$\frac{W(x)}{U_0} = \frac{(2\pi a h \upsilon_{\phi x} E_x k)(\sin kx - H \cos kx)}{(2\pi a^2 B k^4 + T a k^2 + 2\pi h E_\phi - 2\pi a^2 \omega^2 \rho h)} \ . \tag{31}$$

The boundary conditions on the radial equations are not used to define the equations of motion in the radial direction, therefore the circumferential solution does not conform to the boundary conditions at $x = 0$ and $x = L$. Others (Vinson and Sierakowski, 1987) note that the homogeneous solution to shell equations of motion goes to zero away from either end of the shell. Equations (27) and (31) now define the displacements of the shell in the axial and radial directions.

4. FINITE ELEMENT ANALYSIS

The closed form solutions (equations (27) and (31)) are compared to results obtained using finite element analysis. Finite element analysis is a discretized modeling technique that breaks down the structure into a number of subdomains (elements) (Cook, 1974; Zienkiewicz, 1983). Constitutive equations are applied to each of these elements to develop element equations of motion. These individual equations of motion are then assembled to form a global equation of motion. The global equation of motion is of the form

$$\mathbf{M}\frac{d^2\mathbf{g}_i(t)}{dt^2} + \mathbf{C}\frac{d\mathbf{g}_i(t)}{dt} + \mathbf{K}\mathbf{g}_i(t) = \mathbf{f}(x,t) \ , \tag{32}$$

where **M** is the system mass matrix, **C** is the system damping matrix, **K** is the system stiffness matrix, $\mathbf{g}_i(t)$ is the generalized displacement vector in the ith direction, and **f** is the external forcing function vector. The finite element results displayed here were obtained using ANSYS, which is a general purpose finite element program. Finite element analysis has the advantage of handling material and property discontinuities that are not easily resolved with other numerical techniques. It is also used for comparisons with other experiments and theories to verify results. ANSYS has shell models that are internal; therefore, the equations of motion derived here (equations (11) and (12)) were not input into the finite element program as a basis for analysis (Kohnke, 1987). Although neglected in the development of equations (27) and (31), the effect of dynamic coupling from the radial equation into the longitudinal equation is included in the finite element analysis. It is important to note that the finite element analysis is an approximate numerical technique; it is extremely different from the analytical solution presented here. A major disadvantage of finite element analysis is its inability to yield closed form solutions; thus, any time a parameter is changed, the entire problem must be resubmitted for analysis. It is also numerically intensive and cannot be implemented easily on small computers.

5. AN ISOTROPIC EXAMPLE

The closed form solutions derived earlier are now analyzed using an isotropic example. Isotropic shells have the elastic modulus and Poisson's ratio in the axial direction equal to the circumferential direction. The shell properties are listed in table 1. These closed form solutions are compared to results derived using finite element analysis. Equations (19) and (20) are identical to equations (11) and (12) for the isotropic example and thus are not considered separately for this case. Figure 2 shows the model results compared to the finite element analysis for the longitudinal (U) displacement, and figure 3 depicts the model results compared to finite element analysis for the radial (W) displacement. The closed form solutions for both the radial and longitudinal displacements are in very good agreement with the finite element analysis. Also, as predicted by equations (27) and (31), the radial resonances are driven by the longitudinal resonances.

Table 1. Shell Properties for Isotropic Example

Geometric Properties	
Length, L	25 m (82 ft)
Response location, x	7 m (23 ft)
Shell radius, a	0.0254 m (1 in)
Shell thickness, h	0.00254 m (0.1 in)
Shell cross-sectional area, A	0.0004054 m^2 (0.6284 in^2)
Material Properties	
Longitudinal modulus, E_x	1×10^9 N/m^2
Circumferential modulus, E_ϕ	1×10^9 N/m^2
Poisson's ratio, $\upsilon_{x\phi}$	0.49 (dimensionless)
Poisson's ratio, $\upsilon_{\phi x}$	0.49 (dimensionless)
Density, ρ	1000 kg/m^3
Testing Properties	
Spring constant ξ at $x = L$	1×10^5 N/m
Shell tension, T	4450 N (1000 lb)

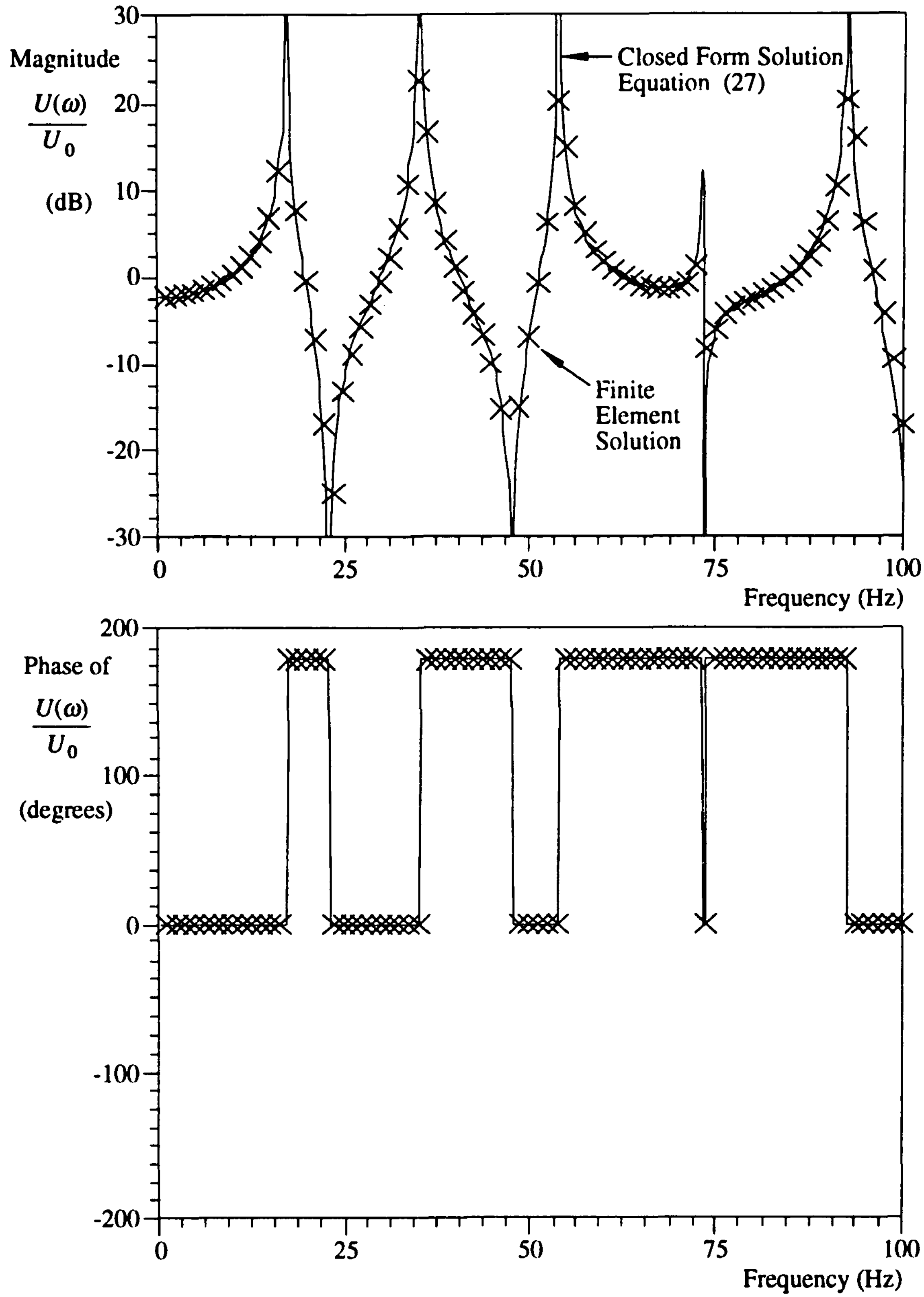

Figure 2. Longitudinal Response of Isotropic Example at $x = 7$ Meters

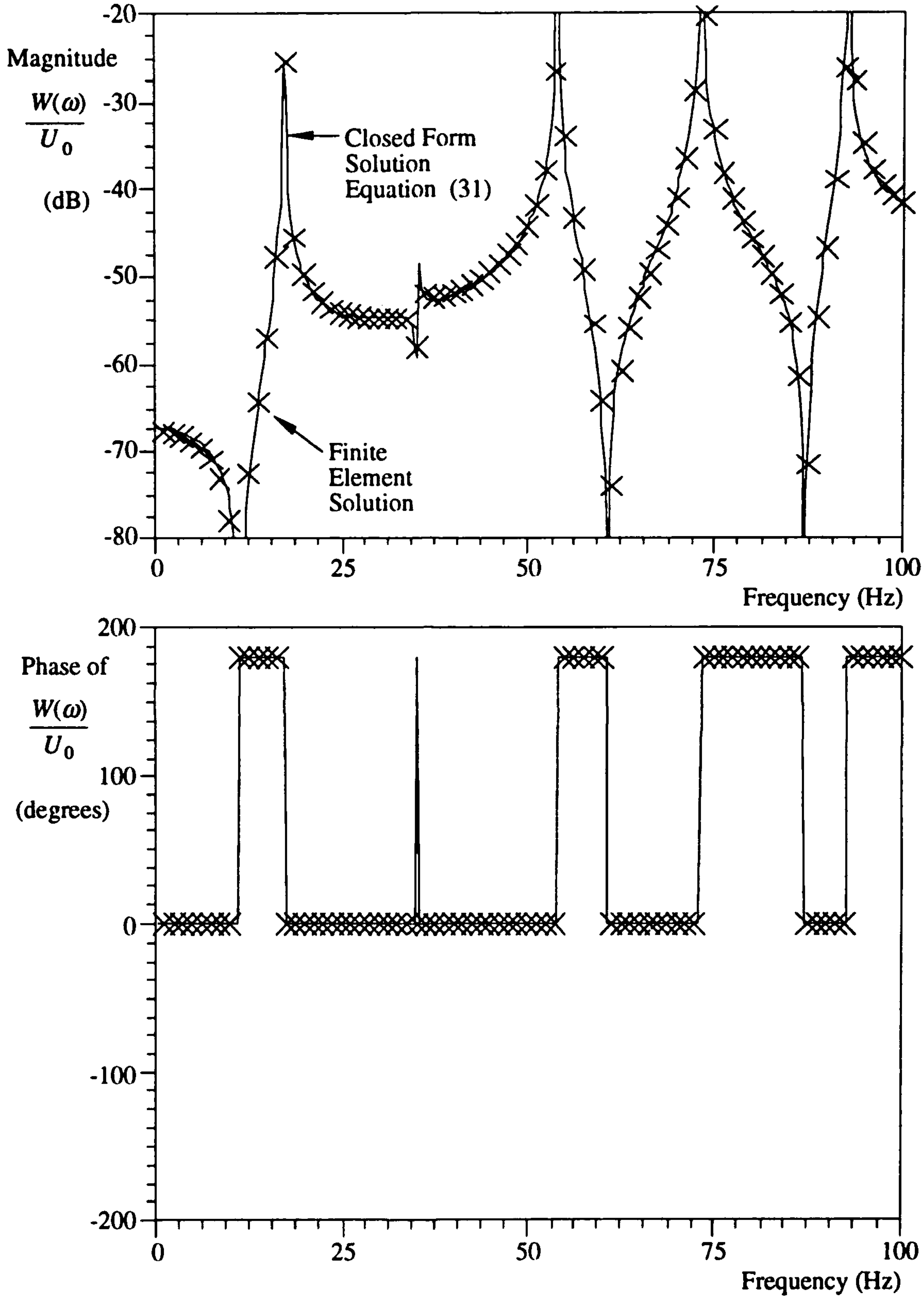

Figure 3. Radial Response of Isotropic Example at $x = 7$ Meters

6. A SPECIALLY ORTHOTROPIC EXAMPLE - FINITE LENGTH SHELL

The closed form solutions are now compared to a specially orthotropic example. Specially orthotropic describes the property where the elastic modulus and Poisson's ratio are different in the radial direction than in the axial direction. This property also requires that the major axis of the material properties be aligned with the circumferential and longitudinal directions of the shell. Specially orthotropic shell properties are listed in table 2. The material properties of a specially orthotropic composite satisfy the equation (Jones, 1975)

$$\frac{\upsilon_{x\phi}}{E_x} = \frac{\upsilon_{\phi x}}{E_\phi} \ . \tag{33}$$

From equation (33), it is evident that the material possesses only three independent parameters. For comparison to equations (27) and (31), the approximate solution technique developed in section 3 can be applied to equations (19) and (20). The solution in the axial direction, which is the same as that developed earlier, is given by equation (27). The equation of motion in the radial direction is

$$\frac{W(x)}{U_0} = \frac{(2\pi a h \upsilon \alpha E_x k)(\sin kx - H\cos kx)}{(2\pi a^2 B k^4 + T a k^2 + 2\pi h E_\phi - 2\pi a^2 \omega^2 \rho h)} \ , \tag{34}$$

where equation (34) is the solution to equation (20). Equation (34), although similar to equation (31), results in a much different radial response of the structure for a specially orthotropic example. Figure 4 shows the model results (equation (27)) compared to finite element analysis for the longitudinal (U) displacement, and figure 5 illustrates the model results (equation (31)) compared to finite element analysis and the model given in equation (34) for the circumferential (W) displacement with $\upsilon = \upsilon_{x\phi}$ used in equation (34). Figure 6 presents the model results (equation (31)) compared to finite element analysis and the model given in equation (34) for the circumferential (w) displacement with $\upsilon = \upsilon_{\phi x}$ in equation (34). The comparison for equation (34) uses both values of Poisson's ratio because the original reference (Chase, 1975) is unclear. It is shown that equation (34) either overestimates or underestimates the structural response depending on the value of Poisson's ratio used. The phase angle of equation (34) is not shown in figures 5 and 6; it is the same as the phase angle of equation (31), therefore it is omitted.

Table 2. Shell Properties for Specially Orthotropic Example

Geometric Properties	
Length, L	25 m (82 ft)
Response location, x	16 m (52.5 ft)
Shell radius, a	0.0254 m (1 in)
Shell thickness, h	0.00254 m (0.1 in)
Shell cross-sectional area, A	0.0004054 m^2 (0.6284 in^2)
Material Properties	
Longitudinal modulus, E_x	1×10^9 N/m^2
Circumferential modulus, E_ϕ	1×10^7 N/m^2
Poisson's ratio, $\upsilon_{x\phi}$	0.4900 (dimensionless)
Poisson's ratio, $\upsilon_{\phi x}$	0.0049 (dimensionless)
Density, ρ	1000 kg/m^3
Testing Properties	
Spring constant ξ at $x = L$	1×10^5 N/m
Shell tension, T	2225 N (500 lb)

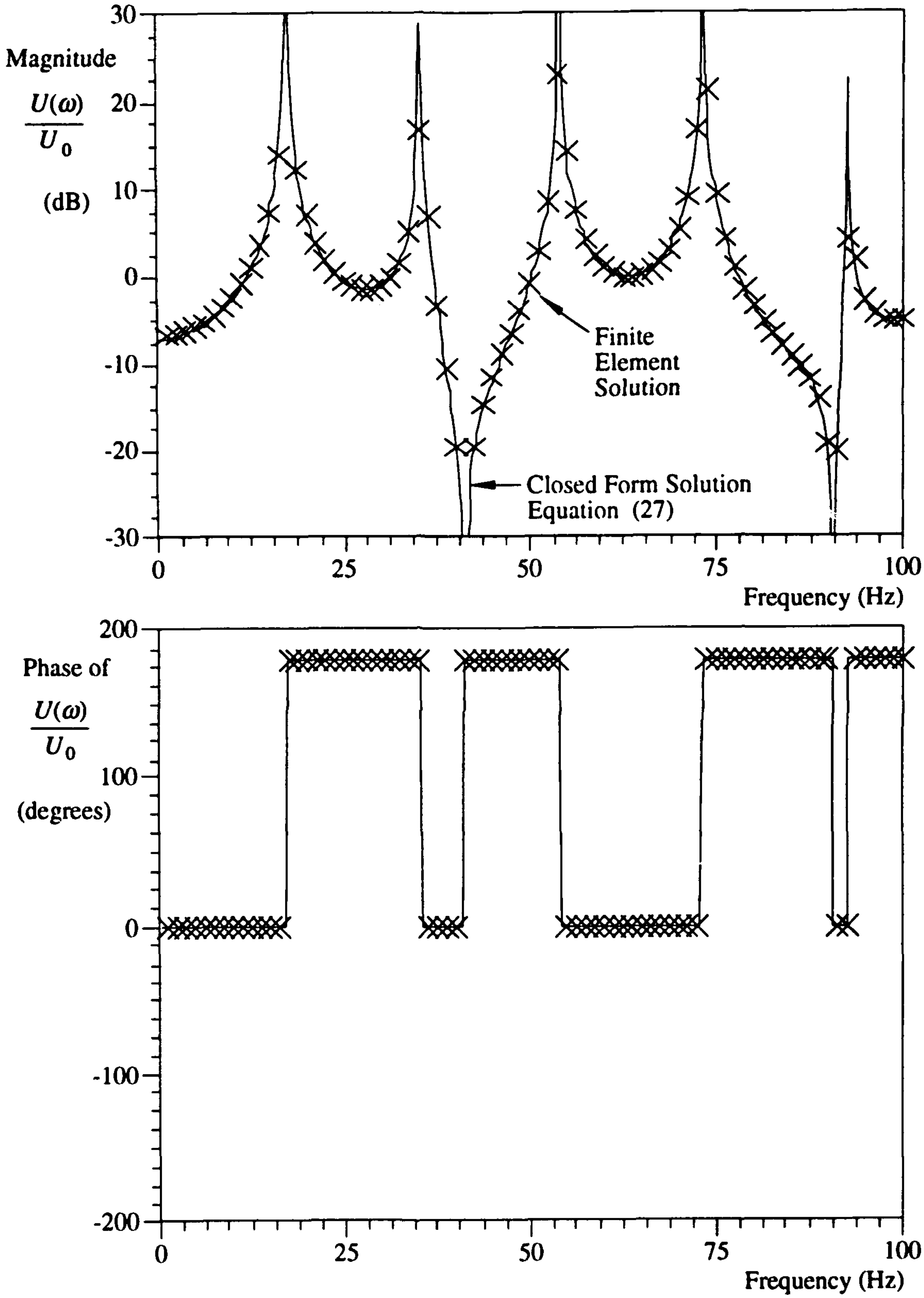

Figure 4. Longitudinal Response of Specially Orthotropic Example at $x = 16$ Meters

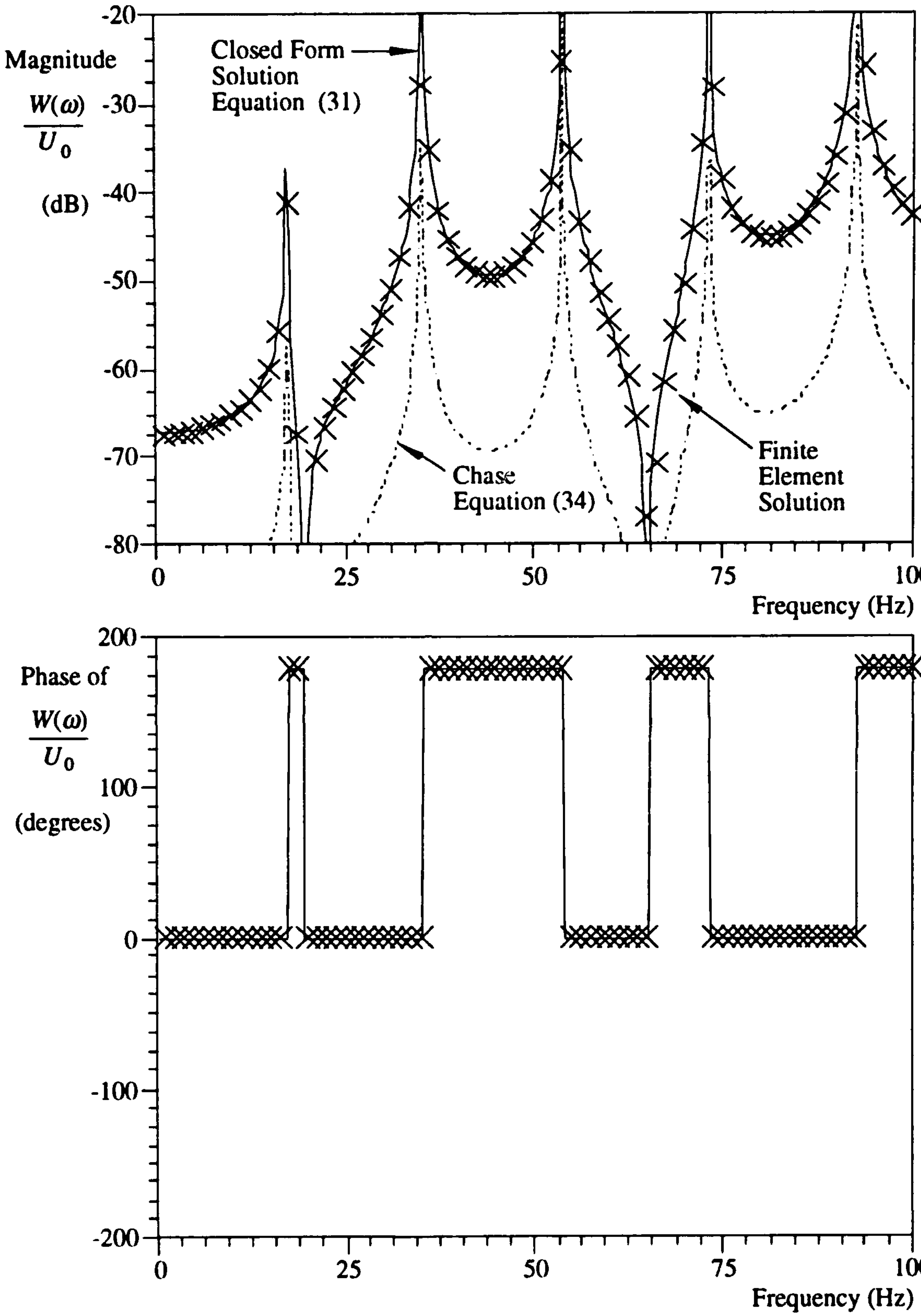

Figure 5. Radial Response of Specially Orthotropic Example at $x = 16$ Meters Using $\upsilon = 0.0049$ for Equation (34)

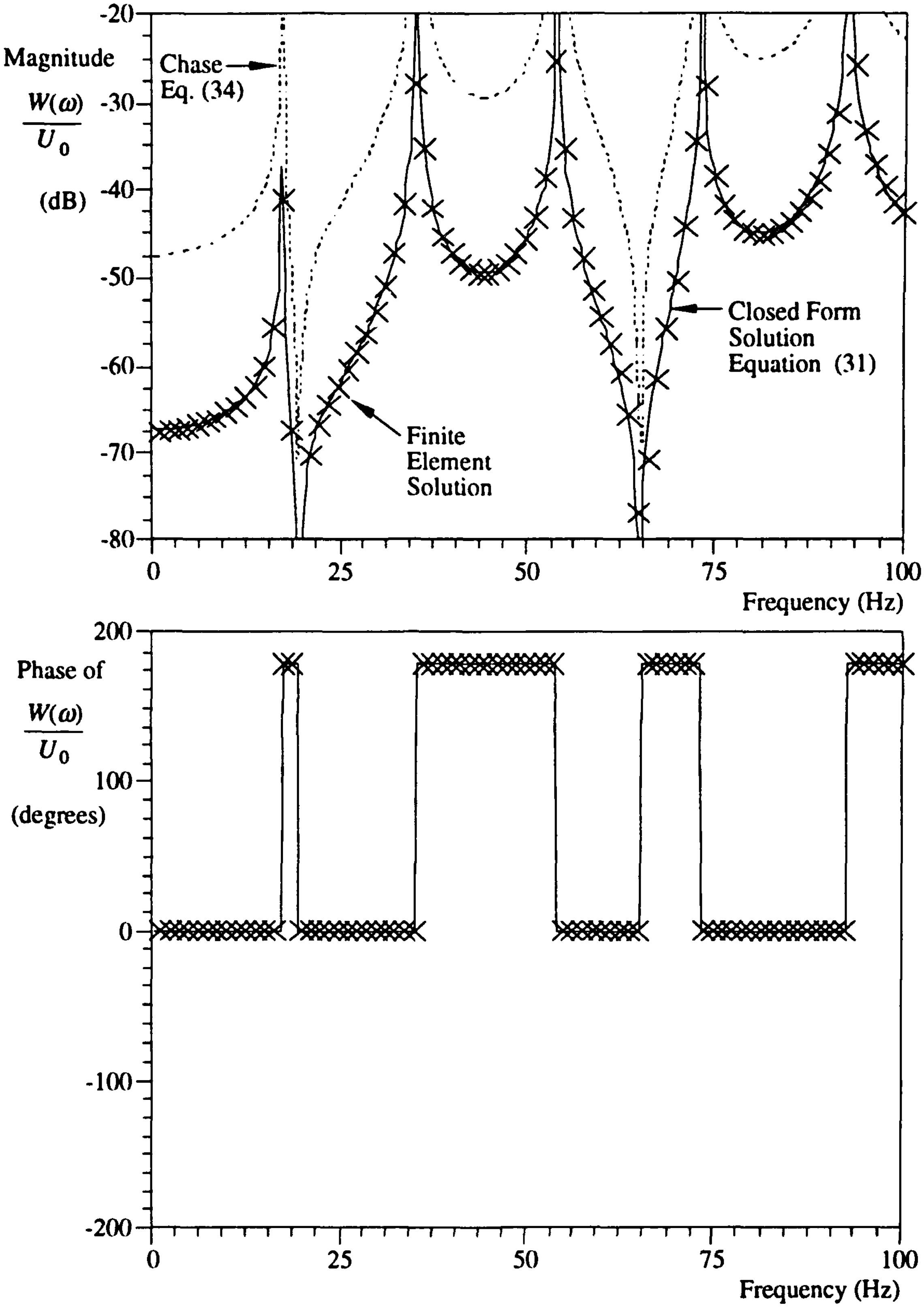

Figure 6. Radial Response of Specially Orthotropic Example at x = 16 Meters Using υ = 0.4900 for Equation (34)

7. A SPECIALLY ORTHOTROPIC EXAMPLE - SEMI-INFINITE LENGTH SHELL

A semi-infinite specially orthotropic shell is now analyzed. This type of analysis is important when the shell is extremely long or when all the energy moving down the shell is absorbed either internally or at the boundary. A convenient way to alter equations (1) through (18) into a semi-infinite system is to change the boundary condition at $x = L$ (equation (14)) to

$$AE_x \frac{\partial u(L,t)}{\partial x} = -c \frac{\partial u(L,t)}{\partial t} , \tag{35}$$

where c now corresponds to a viscous damper (Ns/m) at the end of the shell as depicted in figure 7. It can be shown that a value of (Hull, 1993)

$$c = A\sqrt{\rho E_x} \tag{36}$$

produces a longitudinal response that contains only propagating wave energy. Although the shell has finite length, all the energy moving down the shell will be absorbed by the viscous damper, and the shell response appears as if it is infinitely long. Inserting equation (36) into equation (35) and solving the equations of motion ((11) and (12)) with the boundary condition of equation (13) yields the longitudinal response of

$$\frac{U(x)}{U_0} = e^{-ikx} \tag{37}$$

and the radial response of

$$\frac{W(x)}{U_0} = \frac{(2\pi ah\upsilon_{\phi x} E_x ik)e^{-ikx}}{(2\pi a^2 Bk^4 + Tak^2 + 2\pi hE_\phi - 2\pi a^2 \omega^2 \rho h)} . \tag{38}$$

Equations (19) and (20) (Chase, 1975) can also be solved using the same viscous boundary at $x = L$. The axial equation of motion is identical to equation (37). The radial equation of motion is

$$\frac{W(x)}{U_0} = \frac{(2\pi ah\upsilon\alpha E_x ik)e^{-ikx}}{(2\pi a^2 Bk^4 + Tak^2 + 2\pi hE_\phi - 2\pi a^2 \omega^2 \rho h)} . \tag{39}$$

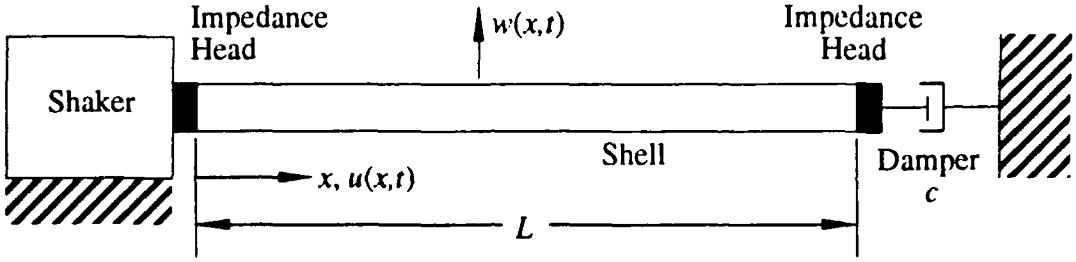

Figure 7. Configuration of Semi-Infinite System

The closed form solutions are now compared for the semi-infinite specially orthotropic shell. The shell properties are listed in table 3. Figure 8 shows the model results (equation (37)) compared to finite element analysis results for the longitudinal (U) displacement. Although a finite length is used in the finite element analysis, the value is also arbitrary. Figure 9 presents the model results (equation (38)) compared to finite element analysis results and the model given in equation (39) for the circumferential (W) displacement with $\upsilon = \upsilon_{x\phi}$. Figure 10 are the model results (equation (38)) compared to finite element analysis results and the model given in equation (39) for the circumferential (W) displacement with $\upsilon = \upsilon_{\phi x}$. The closed form solutions given by equations (37) and (38) agree very well with results from finite element analysis. As in the previous example, equation (39) either overestimates the response or underestimates the response, depending on the value of Poisson's ratio used.

Table 3. Shell Properties for Specially Orthotropic Semi-Infinite Length Example

Geometric Properties	
Length, L	Semi-infinite
Response location, x	12 m
Shell radius, a	0.0254 m (1 in)
Shell thickness, h	0.00254 m (0.1 in)
Shell cross-sectional area, A	0.0004054 m^2 (0.6284 in^2)
Material Properties	
Longitudinal modulus, E_x	1×10^9 N/m^2
Circumferential modulus, E_ϕ	1×10^7 N/m^2
Poisson's ratio, $\upsilon_{x\phi}$	0.4900 (dimensionless)
Poisson's ratio, $\upsilon_{\phi x}$	0.0049 (dimensionless)
Density, ρ	1000 kg/m^3
Testing Properties	
Damper constant c at $x = L$	405.4 Ns/m
Shell tension, T	2225 N (500 lb)

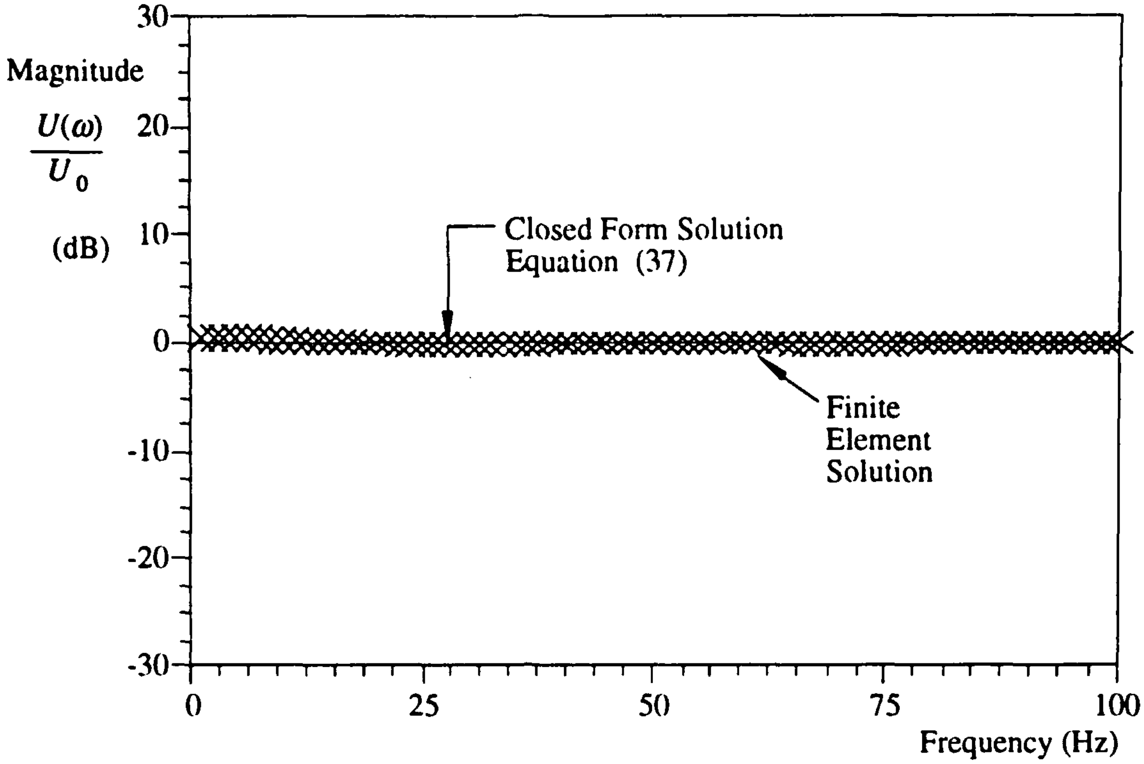

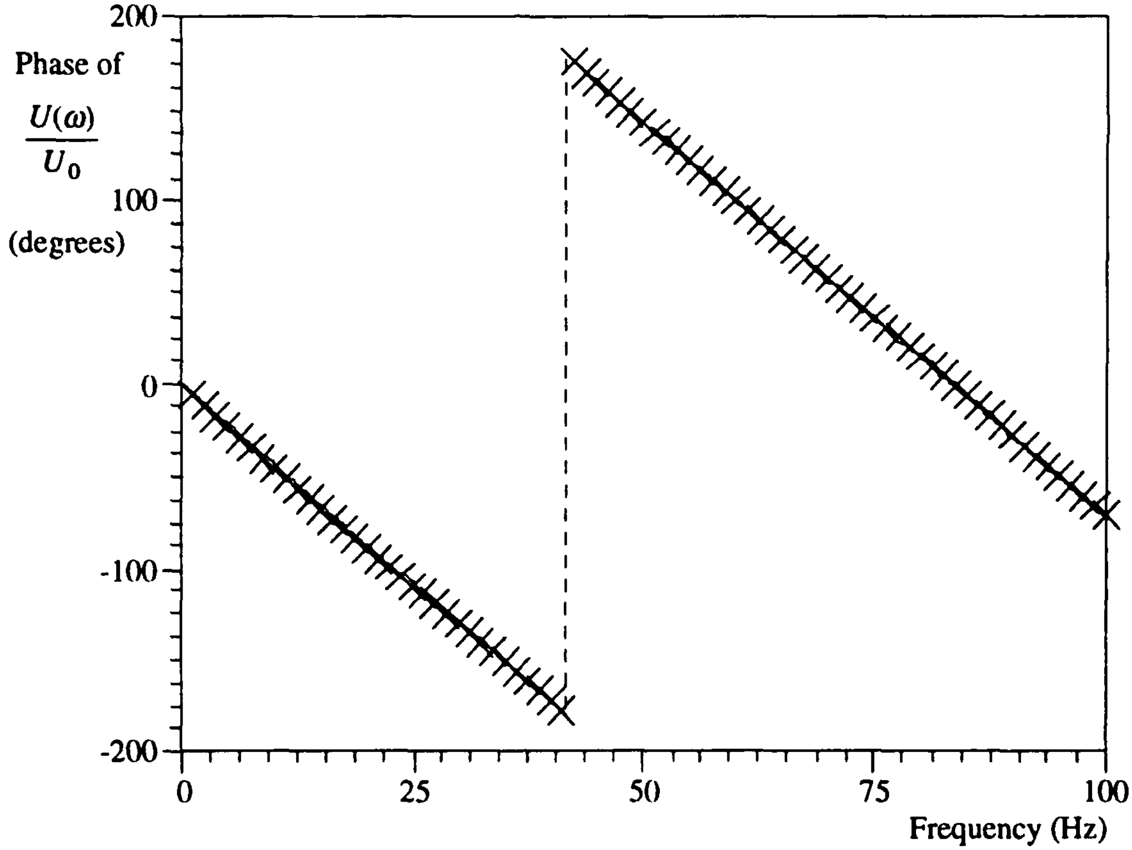

Figure 8. Longitudinal Response of Semi-Infinite Specially Orthotropic Example at x = 12 Meters

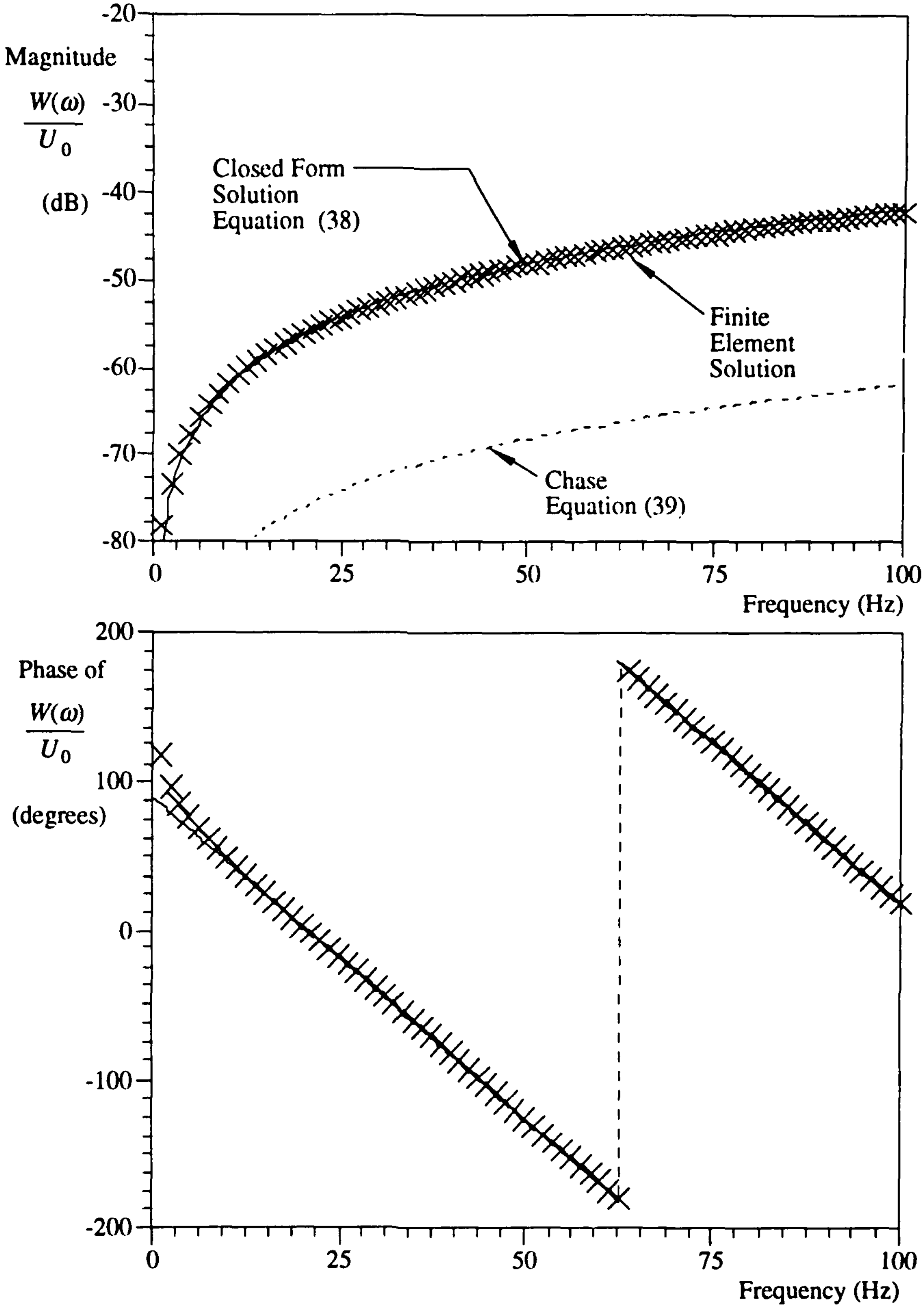

Figure 9. Radial Response of Semi-Infinite Specially Orthotropic Example at $x = 12$ Meters Using $\upsilon = 0.0049$ for Equation (39)

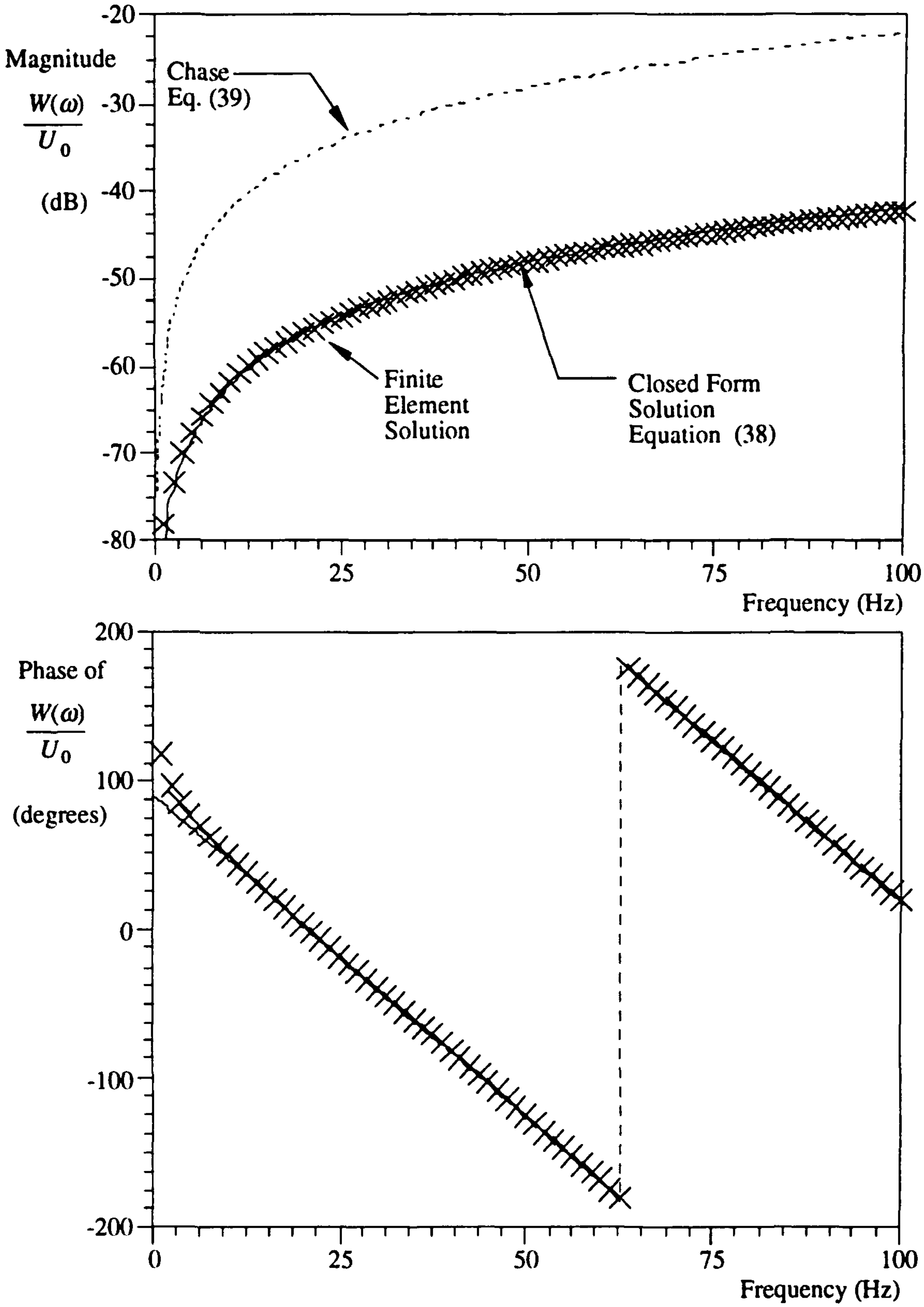

Figure 10. Radial Response of Semi-Infinite Specially Orthotropic Example at $x = 12$ Meters Using $\upsilon = 0.4900$ for Equation (39)

8. A SPECIALLY ORTHOTROPIC EXAMPLE - INCLUSION OF STRUCTURAL DAMPING

The model can include structural damping by changing the elastic modulus from a real-valued term to a complex-valued term. The damping is modeled as an (imaginary) loss modulus with the (real) storage modulus. The shell properties for this damped example are listed in table 4. Except for the addition of damping, these properties are the same as those used for the example in section 6. Figure 11 shows the damped model results compared to the undamped model results for the longitudinal (U) displacement, and figure 12 illustrates the damped model results compared to the undamped model results for the circumferential (W) displacement. ANSYS does not have the capability to model specially orthotropic materials with varying damping coefficients in different directions; therefore, no comparison to finite element analysis is included here. If equation (20) were compared to this example, the difference would be similar to that shown in figures 5 and 6. The results from figures 11 and 12 show that the addition of damping reduces the levels of shell resonance and increases the levels of shell antiresonance. The transfer function is otherwise very similar to the undamped example. The effect of damping would be greater if the shell were longer, because the point harmonic forcing function would be absorbed by a larger medium.

Table 4. Shell Properties for Specially Orthotropic Damped Example

Geometric Properties	
Length, L	25 m
Response location, x	16 m
Shell radius, a	0.0254 m (1 in)
Shell thickness, h	0.00254 m (0.1 in)
Shell cross-sectional area, A	0.0004054 m^2 (0.6284 in^2)
Material Properties	
Longitudinal modulus, E_x	$1 \times 10^9(1+0.05i)$ N/m^2
Circumferential modulus, E_ϕ	$1 \times 10^7(1+0.20i)$ N/m^2
Poisson's ratio, $\upsilon_{x\phi}$	0.4900 (dimensionless)
Poisson's ratio, $\upsilon_{\phi x}$	0.0049 (dimensionless)
Density, ρ	1000 kg/m^3
Testing Properties	
Spring constant ξ at $x = L$	1×10^5 N/m
Shell tension, T	2225 N (500 lb)

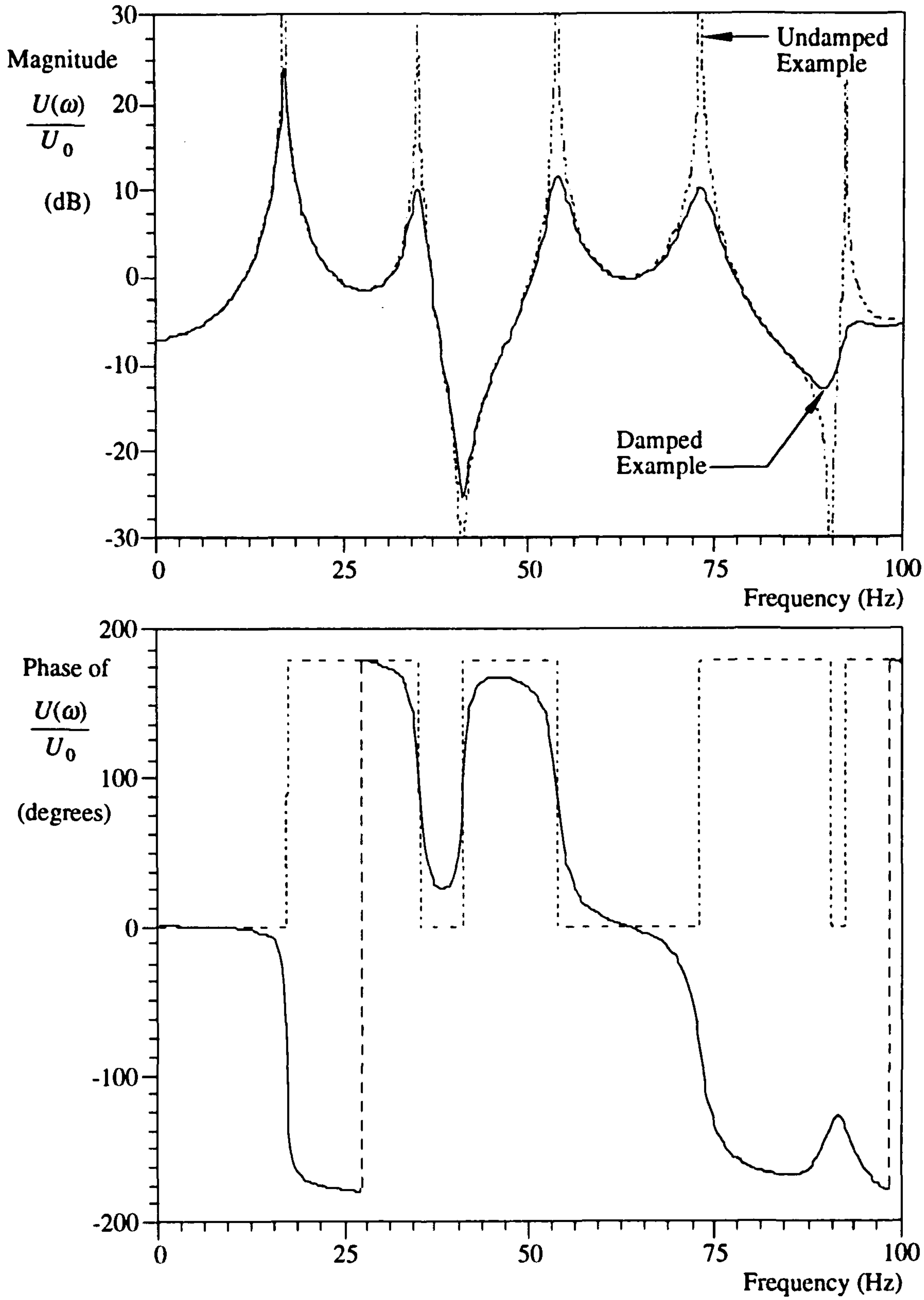

Figure 11. Longitudinal Response of a Damped and Undamped Specially Orthotropic Example at x = 16 Meters

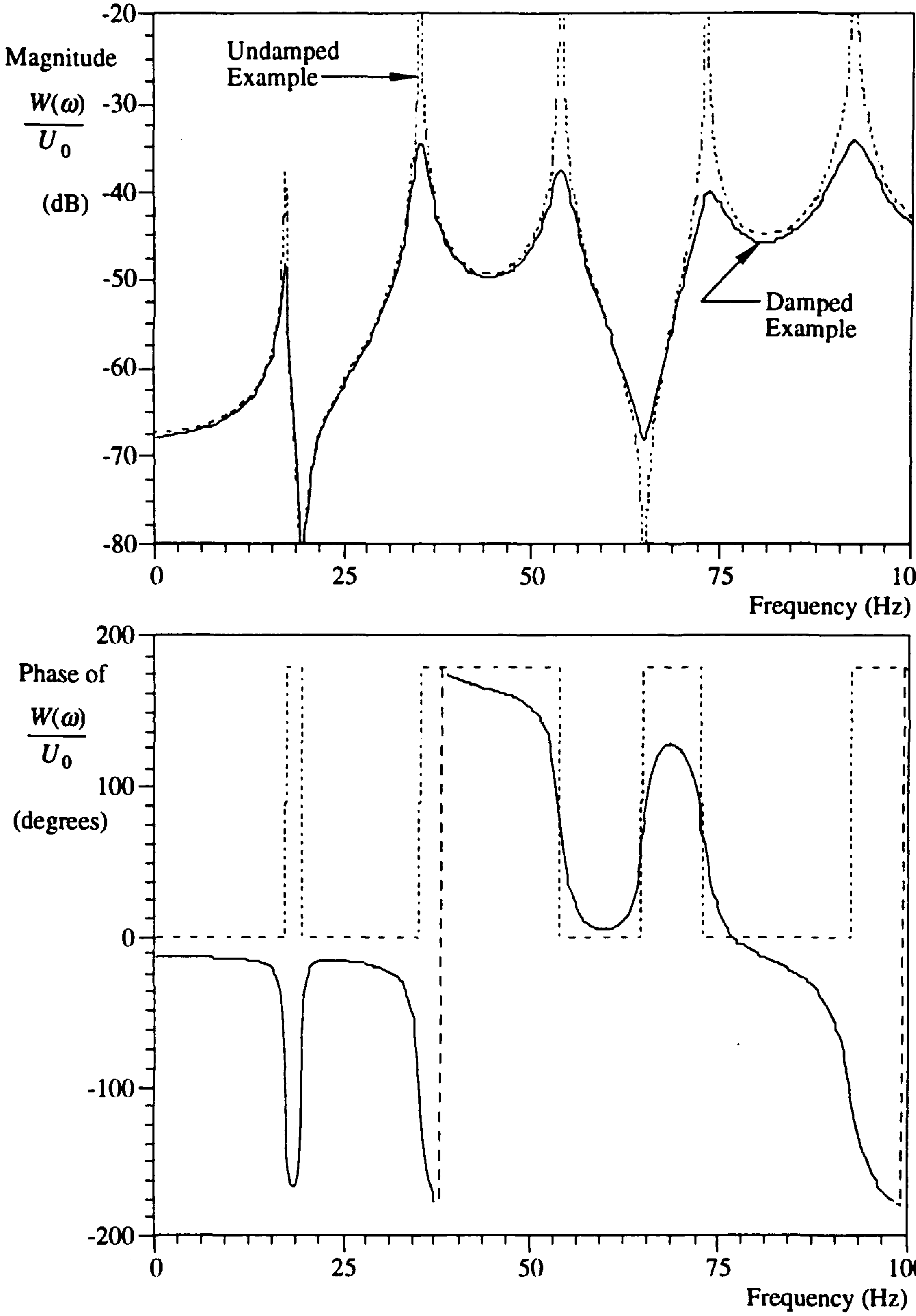

Figure 12. Radial Response of a Damped and Undamped Specially Orthotropic Example at x = 16 Meters

9. DISCUSSION

All the shells modeled in this study compare favorably to finite element theory. The approximate closed form solution is very accurate for a harmonic displacement boundary condition. It is possible that this technique will not be as accurate for other types of forcing or other geometric sizes. The equations previously used to model this system (equations (19) and (20), Chase, 1975) do not produce valid results for specially orthotropic analysis. They can, however, be easily reformulated to conform to the analysis given here. The radial coupling term in equation (19) needs to be altered to

$$\frac{\upsilon \alpha E_x}{a}\frac{\partial w(x,t)}{\partial x} \Rightarrow \frac{\upsilon_{x\phi}\alpha^2 E_x}{a}\frac{\partial w(x,t)}{\partial x}, \tag{39}$$

and the longitudinal coupling term in equation (20) to

$$\frac{h\upsilon \alpha E_x}{a}\frac{\partial u(x,t)}{\partial x} \Rightarrow \frac{h\upsilon_{\phi x} E_x}{a}\frac{\partial u(x,t)}{\partial x}. \tag{40}$$

Such a modification will produce results that are in agreement with the finite element analysis. Note that the larger the difference between the axial and circumferential modulus, the greater is the discrepancy between equations (12) and (20). When the axial modulus equals the circumferential modulus, equation (12) is equal to equation (20).

The nonconforming solution was compared to the finite element solution near the ends of the shell at $x = 0.5$ m and $x = 24.5$ m for the examples listed in sections 5, 6, and 7. These are the two locations in the finite element model that are closest to the end of the shell where a solution can be obtained. The agreement between the finite element model and the closed form approximate solution was similar to that shown earlier. This comparison shows that the radial boundary conditions do not influence the displacements of the shell even 0.5 meters near its end. If the nonconforming solutions were compared to the finite element results at $x = 0$ and $x = L$, the solutions would be similar in the longitudinal direction and dissimilar in the radial directions. This dissimilarity would only be a concern if the solution very close to the end of the shell was of interest.

10. CONCLUSIONS

A nonconforming approximate solution to a thin shell subjected to a harmonic displacement boundary condition was developed in this report. This closed form solution agrees well with finite element solutions for the several models evaluated. It is shown that previous governing equations for the case of specially orthotropic shell models are erroneous. These equations can be reformulated to match the analysis here by an alteration in the coupling terms between the radial and longitudinal equations of motion. Future work in this area should include laboratory testing to obtain experimental results.

11. REFERENCES

Cook, R. D., *Concepts and Applications of Finite Element Analysis*, John Wiley & Sons, New York, 1974.

Chase, D. M., "Self-Noise Induced by Longitudinal Vibration in a Towed Array - The Analytical Approach," *USN Journal of Underwater Acoustics*, vol. 26, no. 1, pp. 53-77, 1975.

Hull, A. J., "A Closed Form Solution of a Longitudinal Bar With a Viscous Boundary Condition," *Journal of Sound and Vibration*, to appear vol. 165, no. 1, August 1993.

Jones, R. M., *Mechanics of Composite Materials*, Hemisphere Publishing Corporation, New York, 1975

Junger, M. C., and Feit, D., *Sound, Structures, and Their Interaction*, The MIT Press, Cambridge, Massachusetts, 1986.

Kohnke, P. C., *ANSYS Engineering Analysis System Theoretical Manual*, Swanson Analysis Systems, Inc., Houston, Pennsylvania, 1987.

Flugge, W., *Stresses in Shells*, Springer-Verlag, Berlin, 1960.

Naghdi, P. M., and Berry, J. G., "On the Equations of Motion of Cylindrical Shells," *Journal of Applied Mechanics*, pp. 160-166, June, 1954.

Qaisi, M. I., "Axisymmetrical Acoustic Vibrations of Simply-Supported Cylindrical Shells," *Applied Acoustics*, vol. 26, pp. 33-43, 1989.

Vinson, J. R., and Sierakowski, R. L., *The Behavior of Structures Composed of Composite Materials*, Martinus Nijhoff Publishers, Dordrecht, 1987.

Zienkiewicz, O. C., *The Finite Element Method*, MacGraw-Hill Book Company, New York, 1983.

INITIAL DISTRIBUTION LIST

Addressee	Number of Copies
Applied Measurement Systems, Inc. (J. Diggs)	1
Bolt Beranek Newman Laboratories (P. Jameson)	1
Cambridge Acoustical Association (J. M. Garrelick, J. E. Cole)	2
Campbell-Kronauer Association (C.R. Campbell)	1
Chase, Inc. (D. M. Chase)	1
DTIC	12
Martin Marietta Corporation (C. Kennedy)	1
Michigan State University (C.R. MacCluer)	2
ONT [T. Goldsberry (OCNR-231)]	2
PEO [G. Kent (PMO-409), D. Lechner (PMO-409/41)]	4
Technology Service Corporation (L. W. Brooks)	1